ORIGINAL ARTICLE

JBMR®

Nf1 Haploinsufficiency Alters Myeloid Lineage Commitment and Function, Leading to Deranged Skeletal Homeostasis

Steven D Rhodes,[1,2] Hao Yang,[2,3] Ruizhi Dong,[2,3] Keshav Menon,[2,3] Yongzheng He,[2,3] Zhaomin Li,[2,3] Shi Chen,[2,3] Karl W Staser,[2,3] Li Jiang,[2,3] Xiaohua Wu,[2,3] Xianlin Yang,[2,3] Xianghong Peng,[4] Khalid S Mohammad,[4] Theresa A Guise,[4] Mingjiang Xu,[2,3,5] and Feng-Chun Yang[1]

[1]Department of Anatomy and Cell Biology, Indiana University School of Medicine, Indianapolis, IN, USA
[2]Herman B. Wells Center for Pediatric Research, Indiana University School of Medicine, Indianapolis, IN, USA
[3]Department of Pediatrics, Indiana University School of Medicine, Indianapolis, IN, USA
[4]Endocrinology and Metabolism, Department of Internal Medicine, Indiana University School of Medicine, Indianapolis, IN, USA
[5]Department of Medical and Molecular Genetics, Indiana University School of Medicine, Indianapolis, IN, USA

ABSTRACT

Although nullizygous loss of *NF1* leads to myeloid malignancies, haploinsufficient loss of *NF1* (*Nf1*) has been shown to contribute to osteopenia and osteoporosis which occurs in approximately 50% of neurofibromatosis type 1 (NF1) patients. Bone marrow mononuclear cells of haploinsufficient NF1 patients and $Nf1^{+/-}$ mice exhibit increased osteoclastogenesis and accelerated bone turnover; however, the culprit hematopoietic lineages responsible for perpetuating these osteolytic manifestations have yet to be elucidated. Here we demonstrate that conditional inactivation of a single *Nf1* allele within the myeloid progenitor cell population (*Nf1-LysM*) is necessary and sufficient to promote multiple osteoclast gains-in-function, resulting in enhanced osteoclastogenesis and accelerated osteoclast bone lytic activity in response to proresorptive challenge in vivo. Surprisingly, mice conditionally *Nf1* heterozygous in mature, terminally differentiated osteoclasts (*Nf1-Ctsk*) do not exhibit any of these skeletal phenotypes, indicating a critical requirement for *Nf1* haploinsufficiency at a more primitive/progenitor stage of myeloid development in perpetuating osteolytic activity. We further identified p21Ras-dependent hyperphosphorylation of Pu.1 within the nucleus of *Nf1* haploinsufficient myelomonocytic osteoclast precursors, providing a novel therapeutic target for the potential treatment of NF1 associated osteolytic manifestations. © 2015 American Society for Bone and Mineral Research.

KEY WORDS: GENETIC ANIMAL MODELS < ANIMAL MODELS; OSTEOCLASTS < CELLS OF BONE; OSTEOPOROSIS < DISEASES AND DISORDERS OF/RELATED TO BONE

Introduction

Myelomonocytic precursor cells give rise to multinucleated, bone resorptive osteoclasts (OCs).[1] The physiologic lineage commitment of monocyte-macrophage precursor cells is pivotal to maintain skeletal homeostasis. Deregulated OC differentiation, recruitment, and/or function can result in either osteoporosis or osteopetrosis,[2,3] affecting not only the skeleton but also altering the bone marrow niche.[4–6] The cytokines macrophage–colony stimulating factor (M-CSF)[7] and receptor activator of nuclear factor κB ligand (RANKL)[8,9] are indispensable for macrophage and OC development, respectively. O*p/op* mice lacking M-CSF exhibit severe osteopetrosis due to an absence of both OCs and macrophages. Adoptive transfer of wild-type (WT) hematopoietic cells is insufficient to correct osteopetrotic phenotypes in *op/op* recipient mice,[10] suggesting that the failure of macrophage and OC differentiation in *op/op* mice is contingent on the extrinsic absence of M-CSF as opposed to intrinsic deficits in either the M-CSF receptor (c-Fms) or intracellular signaling effectors. By contrast, hypersensitivity of macrophages to M-CSF and RANKL in *SHIP*-deficient mice has been shown to result in osteoporosis.[11]

Mutations in the NF1 tumor suppressor gene lead to malignant and nonmalignant disease manifestations of neurofibromatosis type I (NF1), including cutaneous and plexiform neurofibromas, optic nerve gliomas, malignant peripheral nerve sheath tumors (MPNSTs), juvenile myelomonocytic leukemia (JMML), cognitive impairment, cardiovascular disease, and skeletal defects.[12] Neurofibromin, the protein encoded by *NF1*, functions as a GTPase-activation protein (GAP) for Ras, negatively regulating its functional activity.[13] Experimental data now indicates that *Nf1* gene dose (*Nf1* haploinsufficiency)

Received in original form November 20, 2014; revised form April 7, 2015; accepted April 17, 2015. Accepted manuscript online April 27, 2015.
Address correspondence to: Feng-Chun Yang, MD, PhD, Indiana University School of Medicine, Cancer Research Institute, 1044 W. Walnut St., Building R4, Room 427, Indianapolis, IN 46202, USA. E-mail: fyang@iupui.edu
Additional Supporting Information may be found in the online version of this article.

Journal of Bone and Mineral Research, Vol. 30, No. 10, October 2015, pp 1840–1851
DOI: 10.1002/jbmr.2538
© 2015 American Society for Bone and Mineral Research

in hematopoietic-derived cells plays a pivotal role in multiple NF1-associated phenotypes including plexiform neurofibromas, neointima formation, and the skeletal anomalies osteopenia and osteoporosis.[14]

Clinical studies demonstrate that approximately 50% of the NF1 patient population suffers from osteopenia or osteoporosis,[15–20] resulting in significantly increased rates of long-bone fracture.[20,21] Mononuclear cells cultured from the peripheral blood of NF1 patients and the bone marrow of *Nf1*$^{+/-}$ mice exhibit increased OC differentiation and bone resorptive capacity in vitro.[22–24] However, the functional requirement for *Nf1* haploinsufficiency in perpetuating these osteolytic manifestations has yet to be elucidated in a stepwise and lineage-restricted fashion within the hematopoietic compartment. Although *Nf1*$^{+/-}$ myelomonocytic OC progenitor cells exhibit intrinsic, p21-Ras–dependent and PI3K-dependent hypersensitivity to M-CSF and RANKL,[22] the putative contribution of extrinsic alterations in cytokine levels within the *Nf1*-deficient bone microenvironment is difficult to segregate as a confounding factor. For instance, hypersecretion of osteopontin (OPN),[25] transforming growth factor-beta1 (TGF-β1),[26] and RANKL[27] by *Nf1*-null osteoprogenitor cells, together with the decreased expression of the RANKL decoy receptor, osteoprotegerin (OPG),[27] have each been implicated as potential paracrine factors perpetuating osteolytic activity in murine models of the disease.

To understand the cell autonomous and stepwise role of the *Nf1* gene dose in regulating myeloid lineage commitment and OC differentiation, we generated *Nf1-LysM* and *Nf1-Ctsk* mice harboring conditional inactivation of a single *Nf1* allele in myeloid progenitor (MP) cells[28] and mature OCs,[29] respectively. Here we demonstrate that haploinsufficient loss of *Nf1* within MP cells is necessary and sufficient to perpetuate multiple OC gains-in-function both in vitro and in vivo, reminiscent of the phenotype of *Nf1*$^{+/-}$ mice.[22] We further delineate a mechanism by which p21-Ras hyperactivation results in accumulation of phosphorylated Pu.1 within the nucleus of myelomonocytic OC precursors, which may be associated with enhanced osteoclastogenesis, and provide a novel therapeutic target for the potential treatment of NF1 associated osteolytic manifestations.

Materials and Methods

Animals

Nf1-floxed (*Nf1*$^{flox/flox}$) mice were generated in the laboratory of Dr. Luis Parada (University of Texas Southwestern Medical Center) as described.[30] *LysMCre* mice, generated by Dr. Irmgard Forster (University of Duesseldorf),[28] and *CtskCre* mice, generated by Dr. R.A. Davey (University of Melbourne, Australia),[29] were obtained from the Jackson Laboratory (Bar Harbor, ME, USA). Breeding of *Nf1*$^{flox/flox}$ mice with *LysMCre* and *CtskCre* mice yielded *LysMCre;Nf1*$^{flox/+}$ and *CtskCre;Nf1*$^{flox/+}$ mice (abbreviated respectively as *Nf1-LysM* and *Nf1-Ctsk* throughout), which were maintained at the Indiana University School of Medicine in accordance with the Institutional Animal Care and Use Committee and Institutional Review Board guidelines. Cre-mediated recombination of the floxed *Nf1* allele was validated by PCR and Western blot (Supplemental Fig. 1A–C). The genotype of WT mice was either *Nf1*$^{flox/flox}$;*Cre*$^{(-)}$ or *Nf1*$^{flox/+}$;*Cre*$^{(-)}$ for each colony. For all experiments, WT mice were obtained from the same colony as the corresponding mutant mice.

Bone marrow isolation

Bone marrow was flushed from the femur, tibia, and iliac crest in a 5-mL volume of Iscove's Modified Dulbecco's Media (IMDM; Gibco/Invitrogen), supplemented with 1% fetal bovine serum (FBS; Hyclone, ThermoScientific) using a 1.5-inch, 23G needle. Low-density bone marrow mononuclear cells (BMMNCs) were isolated by density gradient centrifugation for 30 min at 700 × g (gh-3.8 rotor; Beckman Coulter) on a 3.5-mL volume of Histopaque (Sigma). The buffy coat layer was collected and washed with IMDM or other media prior to further assays.

Colonogenic progenitor assays

To determine the frequency of MPs in bone marrow, colony-forming unit-macrophage/monocyte (CFU-M) of BMMNCs were performed by seeding 2.5×10^4 BMMNCs into 35-mm gridded dishes containing methylcellulose supplemented with varying doses of murine recombinant M-CSF (0.1, 1, 10, and 50 ng/mL) for 7 days at 37 °C in a 5% CO_2 incubator.[22] Colony type and numbers were counted on an inverted light microscope.

OC differentiation

Murine OCs were cultured in vitro from mouse BMMNCs as described[22] using α-MEM medium supplemented with 10% FBS in the presence of murine recombinant M-CSF (30 ng/mL) and murine recombinant receptor activator of nuclear factor kappa-B ligand (RANKL, 20 ng/mL). On day 3 of culture, the cytokines were changed to M-CSF (30 ng/mL) and RANKL (60 ng/mL) for an additional 3 days of culture. Adherent cells were then fixed and stained for tartrate resistant acid phosphatase (TRACP) according to the manufacturer's instructions (Sigma-Aldrich, USA). TRACP-positive staining OC cells were visualized and photographed with a Nikon TE2000-S microscope (Nikon Inc., Melville, NY, USA) equipped with a QImaging camera (Fryer Company Inc., Cincinnati, OH, USA). Mature OCs were defined as multinucleated TRACP-positive staining cells containing greater than or equal to three nuclei. OC nuclear number and area were scored using NIH ImageJ Software (http://imagej.nih.gov/ij).

Bone resorption assays

BMMNCs were seeded on dentine slices (ALPCO Diagnostic, Windham, NH, USA) and cultured in the presence of M-CSF and RANKL at 37 °C, 5% CO_2 for 7 days. The area of resorptive "pits" was quantified on low power fields using NIH ImageJ Software.

Flow cytometry

BMMNCs were incubated for 45 min at 4 °C with saturating concentrations of anti-mouse antibodies in ~100 μL 3% FBS/0.09% NaN_3 in PBS with 0.25 μg anti-mouse CD16/CD32 ("Fc Block"). For the MP analysis, the following antibodies from BD Biosciences were used: FITC-conjugated anti-lineage markers (CD3, CD4, CD8, B220, Mac1, Gr1, Ter119), anti-CD16/32-PE, anti-CD34-PacificBlue, anti-Sca1-APC-Cy7, and anti-c-Kit-PerCP-Cy5.5. For the mature lineage analysis, the following antibodies from BD Biosciences were used: anti-CD3-FITC, anti-CD8-PacBlue, anti-B220-V500, anti-Mac1-PE, anti-Gr1-PECy7, anti-CD4-APC-Cy7, and anti-CD45.2-PerCP-Cy5.5. Cells were analyzed on an LSR II 407 flow cytometer, and single color compensation controls were acquired using polystyrene microbeads (BD Biosciences). All postacquisition analyses were performed with FlowJo 7.6.3 software (TreeStar, Ashland, OR, USA) with gating parameters determined by fluorescence minus-one controls.

The following gating definitions were used: MPs; granulocyte-monocyte progenitors (GMPs); and megakaryocyte-erythroid progenitors (MEPs). Multipotent progenitor cells (MPPs): $Lin^-Sca1^+c\text{-}Kit^+$. MPs: $Lin^-Sca1^-c\text{-}Kit^+$. Common myeloid progenitors (CMPs): $Lin^-Sca1^-c\text{-}Kit^+CD34^+Fc\gamma RII/II^{-/lo}$. GMPs: $Lin^-Sca1^-c\text{-}Kit^+CD34^+Fc\gamma RII/II^+$. MEPs: $Lin^-Sca1^-c\text{-}Kit^+CD34^-Fc\gamma RII/II^-$. Hematopoietic stem and progenitor cell (HSPCs): $CD150^+Lin^-CD48^-CD41^-Sca1^+c\text{-}Kit^+$. Myeloid cells: $CD3^-B220^-$. Mononuclear cells (Monocytes): $CD3^-B220^-Gr1^-Mac1^+$.

Proresorptive challenge

Twelve-week old, female WT, *Nf1-LysMCre*, and *Nf1-CtskCre* mice underwent either ovariectomy or sham surgery.[22] Briefly, mice were anesthetized using a mixture of ketamine (150 mg/kg) and xylazine (10 mg/kg) administered by intraperitoneal (i.p.) injection. A 2-cm midline dorsal skin incision was performed, followed by incision of the peritoneal cavity to identify and excise the ovaries. Bone mineral density (BMD) was measured once prior to surgery and again after 6 weeks to track the percent change in BMD over time. The mice were subsequently euthanized and the long bones were dissected for further analysis by micro–computed tomography (μCT) and histological methods described below. The cohort sizes of the experimental (OVX) and sham-operated control groups were chosen to achieve sufficient statistical power to detect a significant difference in BMD between genotypes within treatment groups 6 weeks post-surgery, according to our previously published work.[22]

Peripheral dual-energy X-ray absorptiometry

BMD was measured by dual-energy X-ray absorptiometry (DXA) with a Lunar Piximus densitometer (GE Lunar II, Faxitron Corp., Wheeling, IL, USA).[22] Mice were anesthetized with a mixture of ketamine (150 mg/kg) and xylazine (10 mg/kg) injected i.p. Animals were scanned in the prone position with arms and legs extended. A region of interest was defined as the distal femur adjacent to the growth plate (12 × 12 pixels). For OVX experiments, the percent change in BMD was determined by comparing the initial measurement with an endpoint scan, acquired 6 weeks following OVX or sham surgery.

μCT

Formalin fixed femurs were placed in the gantry of a VivaCT 40 μCT scanner (Scanco Medical AG, Bassersdorf, Switzerland). Images were acquired at 55 kV and 145 mA with a voxel size of 10.5 μm. A region of interest was defined as 100 transverse CT slices beginning 250 μm away from the growth plate and extending proximally. Fractional bone volume (BV/TV, %) and architectural properties of trabecular reconstructions: trabecular thickness (Tb.Th, μm), trabecular number (Tb.N, mm^{-1}), trabecular spacing (Tb.Sp, 1/mm), and connectivity density (Conn.D, mm^{-3}) were calculated as described.[31]

Quantitative histomorphometry

Tissues were fixed in 10% formalin for 48 hours, demineralized for 2 weeks in 10% EDTA, and embedded in paraffin. Then, 3.5-μm-thick longitudinal sections were cut using a rotary microtome (Leica). Trabecular BV/TV of the secondary spongiosa and osteoblast number (N.Ob/BS) normalized to the bone surface were quantified on H&E stained sections of the distal femur at ×200 magnification using BIOQUANT OSTEO v11.2 software (BIOQUANT Image Analysis Inc., Nashville, TN, USA). In a similar fashion, number of OCs normalized to the bone surface (N.Oc/BS) was quantified on TRACP-stained sections at ×200 magnification.

Western blotting

Following stimulation with M-CSF, RANKL, and various inhibitors, nuclear and cytoplasmic protein fractions were harvested using a Nuclear/Cytosol Fractionation kit (Biovision, San Francisco, CA, USA). Isolated proteins were fractionated using NuPAGE 4-12% Bis-Tris Gels (Invitrogen) and electrotransferred to polyvinylidene fluoride (PVDF) membranes. Immunoblots were carried out using antibodies specific to Pu.1 (Abcam) and β-actin (Sigma). After incubation with anti-rabbit IgG or anti-mouse IgG (GE Healthcare) antibodies conjugated with horseradish peroxidase (HRP), signals were detected using ECL chemiluminescence substrate (ECL Prime; GE Healthcare). Intensity of bands was determined using ImageJ software.

Phosphatase treatments

Nuclear protein lysates were isolated from $Nf1^{+/-}$ OC progenitor cells after 12 hours stimulation with M-CSF (30 ng/mL) and RANKL (30 ng/mL). Potato acid phosphatase (Sigma) was reconstituted at a concentration of 0.05 U/μL. Heat activation was performed by heating the reconstituted phosphatase to 100 °C for 15 to 20 min prior to incubation with nuclear protein lysates. Phosphatase treatments were performed by adding 0.05 U of either active or heat-inactivated phosphatase to nuclear protein lysates, which were incubated at 37 °C for a duration of 30 min. SDS was subsequently added to each sample, followed by heating to 100 °C for 10 min to quench the reaction prior to Western blotting.

Statistical analysis

Differences between experimental groups were interrogated using the Student's *t* test or either one-factor or two-factor analysis of variance (ANOVA) as appropriate. In the instances where the ANOVA was significant, post hoc testing was performed between individual groups using the Newman-Keuls multiple comparison test. An alpha level of 5% was set as the type I error rate for all studies, with p values <0.05 required to reject the null-hypothesis.

Results

Conditional *Nf1* haploinsufficiency in MP cells promotes expansion of the OC precursor pool, enhancing OC maturation and bone lytic activity

Osteoclastogenesis is a dynamic process requiring the commitment and proliferation of early MPs, followed by terminal myelomonocytic differentiation, and ultimately fusion to multinucleated OCs with bone resorptive activity.[1] Mononuclear cells harvested from the bone marrow of $Nf1^{+/-}$ mice and peripheral blood of human NF1 patients exhibit an increased propensity for OC differentiation and bone resorption ex vivo due to p21-Ras mediated hypersensitivity to M-CSF and RANKL.[22–24] Yet no genetic study has directly assessed the stage of myeloid or OC differentiation at which *Nf1* haploinsufficiency is permissive of these gains-in-function. To investigate the temporal role of *Nf1* gene dose in regulating early-stage versus late-stage OC development, we began by comparing myeloid

lineage commitment and proliferative capacity of BMMNCs harvested from *Nf1-LysM*, *Nf1-Ctsk*, and WT mice. When BMMNCs isolated from these mice were cultured in semisolid methylcellulose media supplemented with varying concentrations of M-CSF, we found that the number of CFU-Ms per femur were significantly increased in *Nf1-LysM* BMMNCs versus WT with increasing doses of M-CSF (Fig. 1*A*). In a complementary approach, flow cytometric analysis of the bone marrow revealed a significant increase in the frequency of MPs (Fig. 1*B*). Thus, conditional *Nf1* haploinsufficiency in early stage MP cells is sufficient to promote expansion of the OC precursor pool as previously observed in $Nf1^{+/-}$ mice.[22] By contrast, however, when we compared the frequency of CFU-M generated from *Nf1-Ctsk* BMMNCs in M-CSF supplemented methylcellulose culture, we observed no significant difference as compared to the WT control (Supplemental Fig. 2A), indicating that conditional *Nf1* haploinsufficiency restricted to the terminal stages of OC differentiation does not alter the lineage commitment or frequency of more primitive MP cells.

We next sought to assess the capacity of *Nf1-LysM*, *Nf1-Ctsk*, and WT BMMNCs to undergo terminal OC differentiation in response to M-CSF and RANK-L. Given the increased frequency of myelomonocytic OC progenitor cells within the bone marrow of *Nf1-LysM* mice, we hypothesized that BMMNCs harvested from these animals would concordantly exhibit enhanced osteoclastogenesis. Indeed, the number of TRACP-positive staining multinucleated OCs (Fig. 1*C*), number of nuclei per OC, and mean OC size (Fig. 1*D*) were significantly increased in *Nf1-LysM* BMMNC cultures as compared to WT controls, suggesting increased OC progenitor fusion and recapitulating the hallmark features of OC cultures derived from the bone marrow of $Nf1^{+/-}$ mice[22] and the peripheral blood of human NF1 patients.[23,24] Although *Nf1-Ctsk* mice do not exhibit any apparent increase in the frequency of OC progenitors within the bone marrow, we nonetheless reasoned that *Nf1* haploinsufficiency, even restricted to late-stage osteoclastogenesis, might still be sufficient to potentiate OC maturation. As expected, we observed no significant difference in the osteoclastogenic capacity of *Nf1-Ctsk* BMMNCs as compared to WT cultures (Supplemental Fig. 2B), suggesting that *Nf1* haploinsufficiency in the terminal stages of OC development alone is insufficient to potentiate OC differentiation as compared to genetic disruption of a single *Nf1* allele in more primitive MP cells. These data also serve as a negative control to exclude the putative contribution of paracrine factors from *Nf1* heterozygous mature OCs that could act on immature cells of the myeloid lineage to promote terminal differentiation.

A defining morphological feature of mature OCs is the organization of the actin cytoskeleton to form a specialized cell–extracellular matrix that provides the appropriate microenvironment for bone matrix degradation. This complex structure is formed by the coalescence of actin cytoskeletal structures termed podosomes that arrange into identifiable patterns such as clusters, rings, and ultimately belts that constitute a functional sealing zone.[32] Here, we show that compared to WT controls, *Nf1-LysM* OC cultures exhibit significantly higher levels of belt formation (Fig. 1*E*, *F*), another characteristic cellular feature observed in $Nf1^{+/-}$ OCs with increased bone resorptive activity.[33]

To directly assess the functional capacity of OCs to degrade bone matrix, OCs were cultured on dentine slices in the presence of M-CSF and RANK-L to quantify the area of "pits" generated by OC-mediated erosion. Consistent with previous data demonstrating increased bone resorptive capacity of OCs cultured from the $Nf1^{+/-}$ mice,[22] we observed a significant increase in "pit" area on dentine slices seeded with *Nf1-LysM* OCs as compared to WT controls (Fig. 1*G*). Consistent with previous negative findings, *Nf1-Ctsk* OC cultures did not exhibit a significant difference in "pit" resorptive capacity as compared to WT (Supplemental Fig. 2C).

Nf1 haploinsufficiency in MP cells is necessary and sufficient to accentuate osteolytic activity in vivo

Intriguingly, although $Nf1^{+/-}$ OCs exhibit multiple gains-in-function,[22] $Nf1^{+/-}$ mice do not spontaneously exhibit commensurate reductions in bone mass or quality as compared to WT mice.[34] By contrast, we previously demonstrated that the consequences of *Nf1* haploinsufficiency can be unmasked in vivo following OVX-induced proresorptive challenge, whereby $Nf1^{+/-}$ mice lose bone mass at approximately double the rate of WT littermates perpetuated by excess osteolytic activity.[22] To characterize the functional consequences of cell-autonomous *Nf1* haploinsufficiency in MP cells versus terminally differentiated OCs in response to proresorptive stress, we ovariectomized *Nf1-LysM* and *Nf1-Ctsk* mice and monitored changes in their bone mass and BMD as compared to WT controls.

Consistent with previous findings, we observed no significant baseline differences in BMD, bone mass, or trabecular architecture between either *Nf1-LysM* (Supplemental Fig. 3A, B) or *Nf1-Ctsk* mice (Supplemental Fig. 4A, B) versus WT controls. However, following OVX induced proresorptive challenge, the rate of bone loss was significantly increased in *Nf1-LysM*-OVX mice as compared to WT controls. *Nf1-LysM*-OVX mice exhibited a $10.8\% \pm 1.5\%$ (mean $\pm$ SE) reduction in distal femoral BMD during the 6 weeks following OVX surgery versus WT animals, which lost only $6.8\% \pm 0.7\%$ of distal femoral BMD (Fig. 2*B*). As an additional control group, sham-operated animals gained approximately 1% to 3% of femoral BMD over the 6-week time course. Representative μCT reconstructions illustrate the marked loss of trabecular bone in OVX *Nf1-LysM* mice as compared to OVX WT controls (Fig. 2*A*). Corroborating these data, quantitative μCT evaluation revealed significant deficits in femoral BV/TV (Fig. 2*C*), with commensurate changes in multiple bone microarchitecture parameters, including Tb.N, Tb.Th, and Tb.Sp between OVX *Nf1-LysM* and OVX WT mice (Fig. 2*D–F*, respectively). Finally, histomorphometric enumeration of TRACP-positive multinucleated OCs lining the trabecular bone surface revealed significantly increased OC numbers in the femurs of OVX *Nf1-LysM* mice (Fig. 2*G*, *H*), implicating enhanced osteoclastogenesis as the pivotal factor promoting excess bone catabolic activity in *Nf1-LysM* animals.

Intriguingly, when analogous studies were performed in *Nf1-Ctsk* mice, whereby *Nf1* haploinsufficiency is restricted to mature, terminally differentiated OCs, we observed no significant differences in bone mass or microarchitecture parameters when comparing WT-OVX and *Nf1-Ctsk*-OVX mice. Although bone loss occurred in both the mutant and control animals, the percentage reduction in femoral BMD was equivalent between WT-OVX and *Nf1-Ctsk*-OVX mice (Fig. 3*A*). Representative μCT reconstructions illustrate comparable bone loss in the distal femur between ovariectomized WT and *Nf1-Ctsk* mice (Fig. 3*B*). Quantitatively, we detected no significant difference in femoral BV/TV (Fig. 3*C*) or trabecular architecture parameters (Fig. 3*D–I*) when comparing *Nf1-Ctsk* and WT animals following OVX. Collectively, these data imply that conditional *Nf1* haploinsufficiency in mature OCs is insufficient to perpetuate increased osteolytic lytic activity in response proresorptive challenge; but rather, genetic ablation of *Nf1* in more primitive MP cells appears

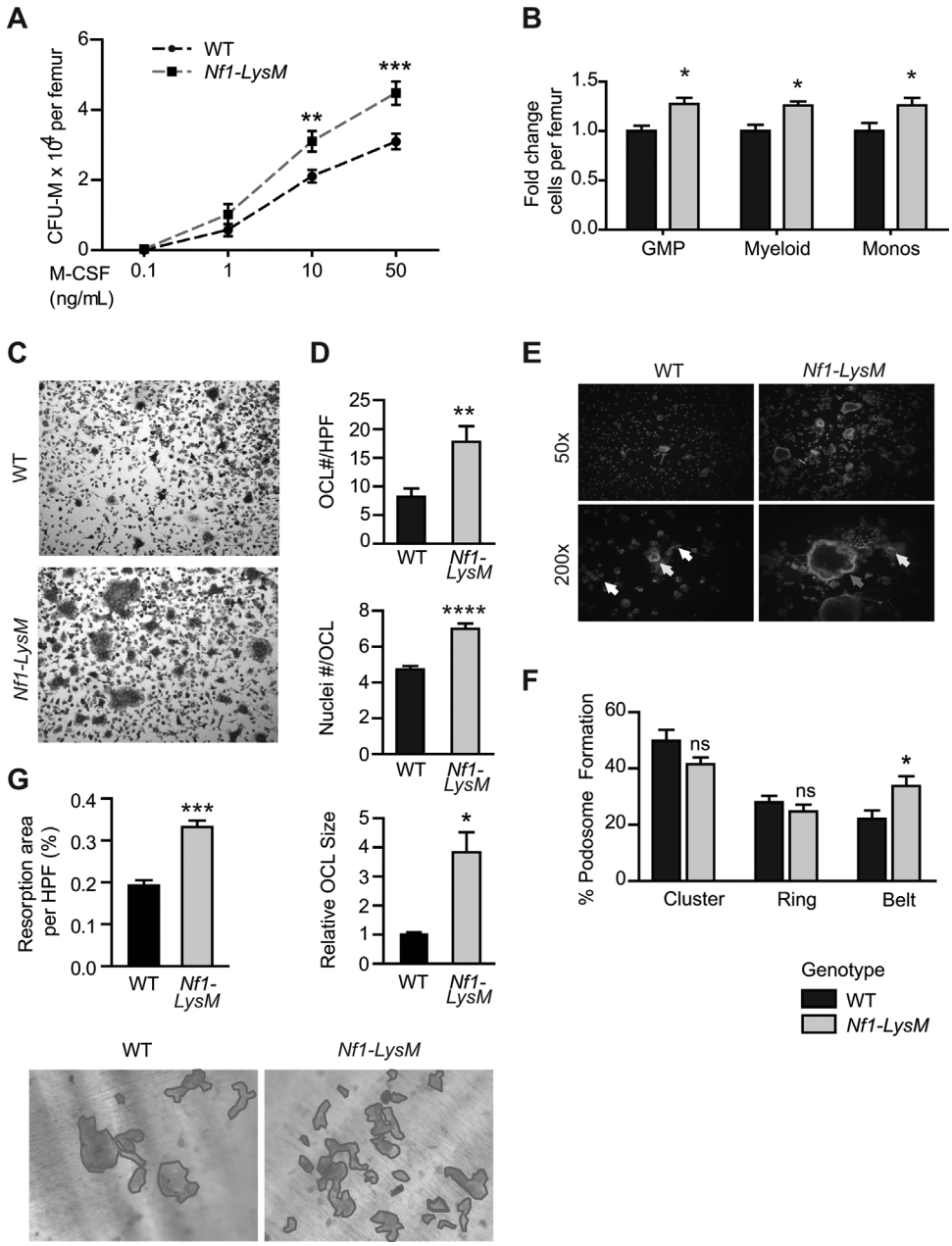

Fig. 1. *Nf1* haploinsufficiency in myeloid progenitor cells promotes expansion of the OC progenitor population and potentates OC differentiation. (*A*) The number of CFU-Ms per femur were enumerated after 7 days culture in semisolid methylcellulose media. $^{**}p < 0.01$, $^{***}p < 0.001$, *Nf1-LysM* versus WT. $n = 8$ mice per genotype. (*B*) Populations of GMP, myeloid cells, and monocytes in the bone marrow were identified by flow cytometry. Fold changes in the number of cells per femur are reported. $^{*}p < 0.05$, *Nf1-LysM* versus WT. $n = 4$ mice per genotype. (*C*) Representative photomicrographs show TRACP staining of bone marrow–derived osteoclasts cultured in the presence of M-CSF and RANKL for 6 days. (*D*) The number of osteoclasts per HPF, the number of nuclei per osteoclast, and the mean osteoclast size were quantitated as shown. $^{*}p < 0.05$, $^{**}p < 0.01$, $^{***}p < 0.001$, *Nf1-LysM* versus WT. $n = 4$ biological replicates per genotype. (*E*) Representative photomicrographs show actin ring formation in bone marrow–derived osteoclast cultures at $\times 50$ (top) and $\times 200$ (bottom) magnification. Cells were stained with Alexa Fluor 488 Phalloidin (green) and Hoechst (blue). (*F*) Podosome formation was evaluated by determining the percent distribution of actin organization into clusters, rings, and belts. $^{*}p < 0.05$, *Nf1-LysM* versus WT. $n = 4$ biological replicates per genotype. (*G*) Osteoclasts were incubated on dentine slices with representative photomicrographs showing resorptive "pits" generated by osteoclast bone lytic activity. Resorptive "pit" area was quantified as shown in the bar graph. $^{***}p < 0.001$, *Nf1-LysM* versus WT. OC = osteoclast; GMP = granulocyte-monocyte progenitor; CFU-M = colony forming unit monocyte/macrophage; TRACP = tartrate-resistant acid phosphatase; HPF = high power field; OCL = osteoclast.

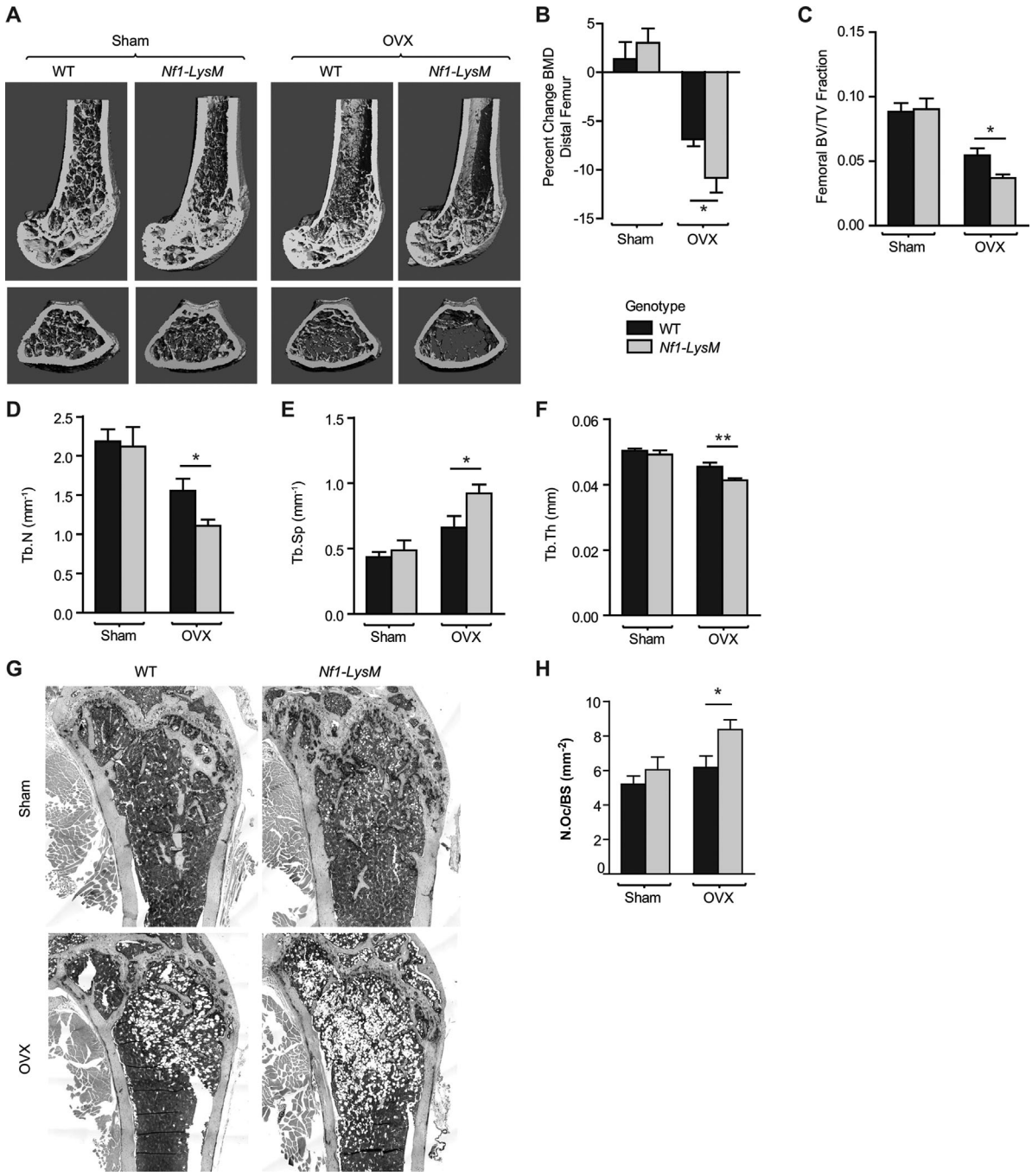

Fig. 2. Conditional *Nf1* haploinsufficiency in myeloid progenitor cells potentiates osteolytic activity in vivo in response to OVX-mediated proresorptive challenge. (*A*) Representative μCT shows reconstructed femora in longitudinal (top) and transverse (bottom) cross-sections 6 weeks postsurgery (OVX versus sham-operated controls). (*B*) The OVX-induced reduction (percentage change) in BMD of the distal femur was determined by pDXA measurements acquired before and 6 weeks after OVX versus sham surgery. *$p < 0.05$, OVX *Nf1-LysM* vs OVX WT. WT Sham ($n = 5$), *Nf1-LysM* Sham ($n = 5$), WT OVX ($n = 8$), *Nf1-LysM* Sham ($n = 10$) mice per genotype. (*C*) Trabecular BV/TV was quantified by μCT. WT Sham ($n = 6$), *Nf1-LysM* Sham ($n = 6$), WT OVX ($n = 7$), *Nf1-LysM* Sham ($n = 12$) mice per genotype. *$p < 0.05$, OVX *Nf1-LysM* vs OVX WT. Trabecular microarchitecture parameters including Tb.N (*D*), Tb.Sp (*E*), and Tb.Th (*F*) were quantified by μCT. WT Sham ($n = 6$), *Nf1-LysM* Sham ($n = 6$), WT OVX ($n = 7$), *Nf1-LysM* Sham ($n = 12$) mice per genotype. *$p <$ 0.05, OVX *Nf1-LysM* vs OVX WT. (*G*) Representative photomicrographs of TRACP-stained distal femora of WT and *Nf1-LysM* mice 6 weeks following either sham or OVX surgery. (*H*) N.Oc/BS were manually enumerated at ×100 magnification on TRACP-stained sections of the distal femur. WT Sham ($n = 5$), *Nf1-LysM* Sham ($n = 5$), WT OVX ($n = 3$), *Nf1-LysM* Sham ($n = 5$) mice per genotype. *$p < 0.05$, OVX *Nf1-LysM* vs OVX WT. OVX = ovariectomized/ovariectomy; μCT = micro–computed tomography; BMD = bone mineral density; pDXA = peripheral dual-energy X-ray absorptiometry; BV/TV = bone volume fraction; Tb.N = trabecular number; Tb.Sp = trabecular spacing; Tb.Th = trabecular thickness; TRACP = tartrate-resistant acid phosphatase; N.Oc/BS = number of osteoclasts per mm^2 bone surface.

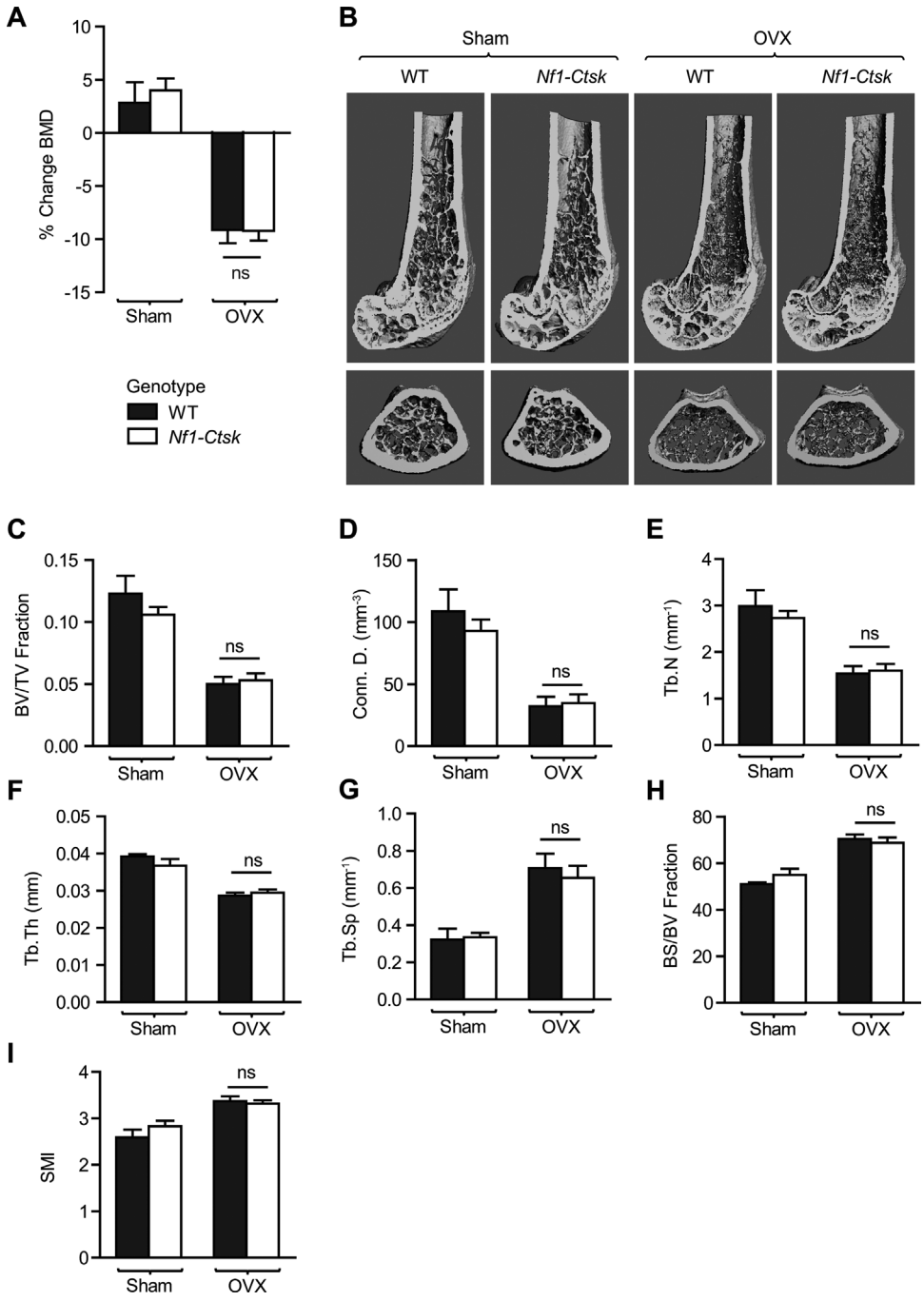

Fig. 3. Conditional *Nf1* heterozygosity in terminally differentiated OCs is not sufficient to potentiate bone catabolic activity in ovariectomized *Nf1-Ctsk* mice. (*A*) The percentage change in BMD 6 weeks post-OVX versus sham surgery was compared between WT and *Nf1-Ctsk* mice. WT Sham ($n = 7$), *Nf1-Ctsk* Sham ($n = 6$), WT OVX ($n = 15$), *Nf1-Ctsk* OVX ($n = 10$) mice per genotype. (*B*) Representative μCT-reconstructed femurs in longitudinal (top) and transverse (bottom) cross-sections for WT versus *Nf1-Ctsk* mice 6 weeks following either sham or OVX surgery. (*C*) Femoral BV/TV was quantified by μCT as shown and revealed no significant difference between WT and *Nf1-Ctsk* mice. WT Sham ($n = 5$), *Nf1-Ctsk* Sham ($n = 5$), WT OVX ($n = 12$), *Nf1-Ctsk* OVX ($n = 12$) mice per genotype. No significant differences in trabecular microarchitecture parameters were found when comparing Conn.D (*D*), Tb.N (*E*), Tb. Th (*F*), Tb.Sp (*G*), BS/BV (*H*), and SMI (*I*) between WT and *Nf1-Ctsk* mice undergoing OVX surgery. WT Sham ($n = 5$), *Nf1-Ctsk* Sham ($n = 5$), WT OVX ($n = 12$), *Nf1-Ctsk* OVX ($n = 12$) mice per genotype. BMD = bone mineral density; OVX = ovariectomized/ovariectomy; ns = no significant difference; BV/TV = bone volume fraction; μCT = micro–computed tomography; Conn.D = connectivity density; Tb.N = trabecular number; Tb.Th = trabecular thickness; Tb.Sp = trabecular spacing; BS/BV = bone surface to bone volume ratio; SMI = structure model index.

to be required to permit expansion of the OC precursor pool within the bone marrow, thereby promoting accelerated bone resorption in vivo.

Previous studies have demonstrated the *LysM*-Cre driver to be relatively specific to primitive myeloid lineages within the hematopoietic compartment.[28] Nevertheless, to further confirm that the observed phenotype in *Nf1-LysM* mice was unrelated to possible ectopic recombination or "leakage" of the *LysM*-Cre driver in the osteoblast lineage, osteoblasts were enumerated on the bone surface in WT and *Nf1-LysM* mice (Supplemental Fig. 3C). We observed no significant difference in the number of osteoblasts per mm^2 bone surface (N.Ob/BS, mm^{-2}) within the distal femur when comparing *Nf1-LysM* mice to the WT control, suggesting that the enhanced bone loss in *Nf1-LysM* mice in response to proresorptive stress is primarily related to increased OC bone lytic activity.

Nf1 haploinsufficiency in OC progenitors results in Ras-dependent accumulation of phosphorylated Pu.1 in the nucleus

Given that haploinsufficient loss of *Nf1* in MP cells is critical to promoting increased osteolytic activity in vivo, we therefore reasoned that neurofibromin may play a pivotal role in regulating the expression and/or activity level of myeloid-dependent transcription factors. Pu.1 transcriptional activity is required for myelomonocytic and OC differentiation, whereby mice lacking Pu.1 exhibit severe osteopetrosis and are deficient in both macrophages and OCs secondary to impaired expression of the M-CSF receptor, c-Fms.[35] Here, we show that the expression level of Pu.1 is increased in the nucleus of *Nf1* haploinsufficient OC progenitors relative to WT controls stained with FITC-labeled anti-Pu.1 (green) and Hoechst (blue) (Fig. 4*A*). We next performed Western blot analysis to examine Pu.1 protein levels in OC progenitors treated with M-CSF and RANKL. When we probed with Pu.1-specific antiserum (Santa Cruz, CA, USA), the predominant protein detected in WT nuclear lysates migrated at an apparent molecular weight of approximately 35 kD. Intriguingly, the expression of two additional bands in the 40-kD to 55-kD range was markedly enriched in the $Nf1^{+/-}$ nuclear lysates across multiple time points (Fig. 4*B*).

Phosphorylation of Pu.1 is known to retard its migration in SDS-PAGE electrophoresis.[36,37] To confirm that these band shifts represent phosphorylated forms of Pu.1, nuclear lysates were treated with potato acid phosphatase prior to electrophoresis. Phosphatase treatment resulted in complete conversion of the shifted bands to the lower molecular weight, unphosphorylated Pu.1 species (Fig. 4*C*). By contrast, treatment of the lysates with heat denatured potato acid phosphatase did not alter the migration or intensity of the shifted bands, thus validating that these bands correspond specifically to phosphorylated Pu.1 species (Fig. 4*C*).

Given neurofibromin's function as a GTPase activating protein (GAP) for p21-Ras, we therefore reasoned that p21-Ras hyperactivation in *Nf1* haploinsufficient OCs may underlie the accumulation of the phosphorylation form of Pu.1 in the nucleus. To test this hypothesis, we transduced primary $Nf1^{+/-}$ c-kit^+ hematopoietic cells with a recombinant retrovirus encoding the full-length *NF1* GAP-related domain (GRD) and a selectable marker, *pac*, which confers resistance to puromycin.[38] As compared to $Nf1^{+/-}$ c-kit^+ cells expressing murine stem cell virus (MSCV)-*pac* alone, reconstitution of the full-length *NF1-GRD* in *Nf1* haploinsufficient c-kit^+ cells significantly attenuated the phosphorylation of nuclear Pu.1 (Fig. 4*D*). Given recent findings implicating Pu.1 phosphorylation in the transcriptional activation of terminal myeloid-specific gene programs,[39,40] we postulate this to be a previously unrecognized mechanism by which *Nf1* haploinsufficiency engenders myeloid lineage commitment, thereby promoting osteoclastogenesis and hyperresorptive activity.

Discussion

OCs cultured ex vivo from the bone marrow of $Nf1^{+/-}$ mice and the peripheral blood of human NF1 patients exhibit multiple gains-in-function,[22–24] consistent with clinical observations that NF1 patients have reduced BMD[15–19,41] and are predisposed to increased fracture risk.[20,21] However, the functional requirement for *Nf1* haploinsufficiency within hematopoietic cells to perpetuate these osteolytic manifestations has yet to be elucidated in a stepwise, lineage-restricted fashion. Here we demonstrate that conditional inactivation of a single *Nf1* allele within the MP cell population (*Nf1-LysM*) is necessary and sufficient to promote multiple OC gains-in-function, resulting in increased OC progenitor fusion, enhanced osteoclastogenesis, and accelerated OC bone lytic activity in response to proresorptive challenge in vivo. Intriguingly, mice conditionally *Nf1* heterozygous in mature, terminally differentiated OCs (*Nf1-Ctsk*) do not recapitulate these phenotypes, indicating a critical requirement for *Nf1* haploinsufficiency at a more primitive stage of myeloid development in perpetuating enhanced osteolytic activity. Given that genetic ablation of a single *Nf1* allele in terminally differentiated OCs alone is insufficient to augment the rate of bone lytic activity, we thus postulate that expansion of the OC precursor pool and an overall increase in OC numbers are the preponderant factors driving bone resorption in the context of *Nf1* haploinsufficiency (Fig. 5).

In contrast to the *Nf1-Ctsk* model, which does not display evidence of OC hyperactivity as observed in *Nf1-LysM* and $Nf1^{+/-}$ animals,[22] Alanne and colleagues[42] recently reported that transgenic mice harboring conditional *Nf1* nullizygous ($Nf1^{-/-}$) OCs driven by *TRAPCre* exhibit increased bone resorptive capacity and aberrant actin ring formation in vitro. Despite differences in *Nf1* gene dose (*Nf1* heterozygosity in *Nf1-Ctsk* mice versus biallelic *Nf1* inactivation in the *TRACPCre;*$Nf1^{flox/flox}$ model), we postulate that the apparent OC gains-in-function in this mouse model are likely due to the expression of *TRAPCre* in more primitive stages of OC/myeloid development as compared to *CtskCre*, which is restricted to mature, terminally differentiated OCs.[29] Supporting this concept, the authors report that *TRACPCre;*$Nf1^{flox/flox}$ mice exhibit a number of extraosseous features including splenomegaly and megakaryocytosis. These findings are reminiscent of the juvenile myelomonocytic leukemia (JMML)-like myeloproliferative disease (MPD) phenotypes seen following *NF1(Nf1)* loss of heterozygosity (LOH) in the hematopoietic compartment,[43,44] and are suggestive of *TRAPCre* recombination of *Nf1* in relatively primitive myeloid OC precursors as reported.[29] Although the physiological relevance of the *Nf1* nullizygosity within the OC lineage remains questionable given that NF1 patients suffering from osteopenia/osteoporosis typically retain one functional *NF1* allele within the hematopoietic compartment, these data nonetheless provide critical insight regarding the stage of myeloid/OC differentiation at which loss of *Nf1* is permissive of OC gains-in-function.

Nf1-LysM BMMNCs exhibit increased CFU-M in methylcellulose culture and enhanced osteoclastogenic capacity in response to M-CSF and RANKL, thereby resulting in accelerated

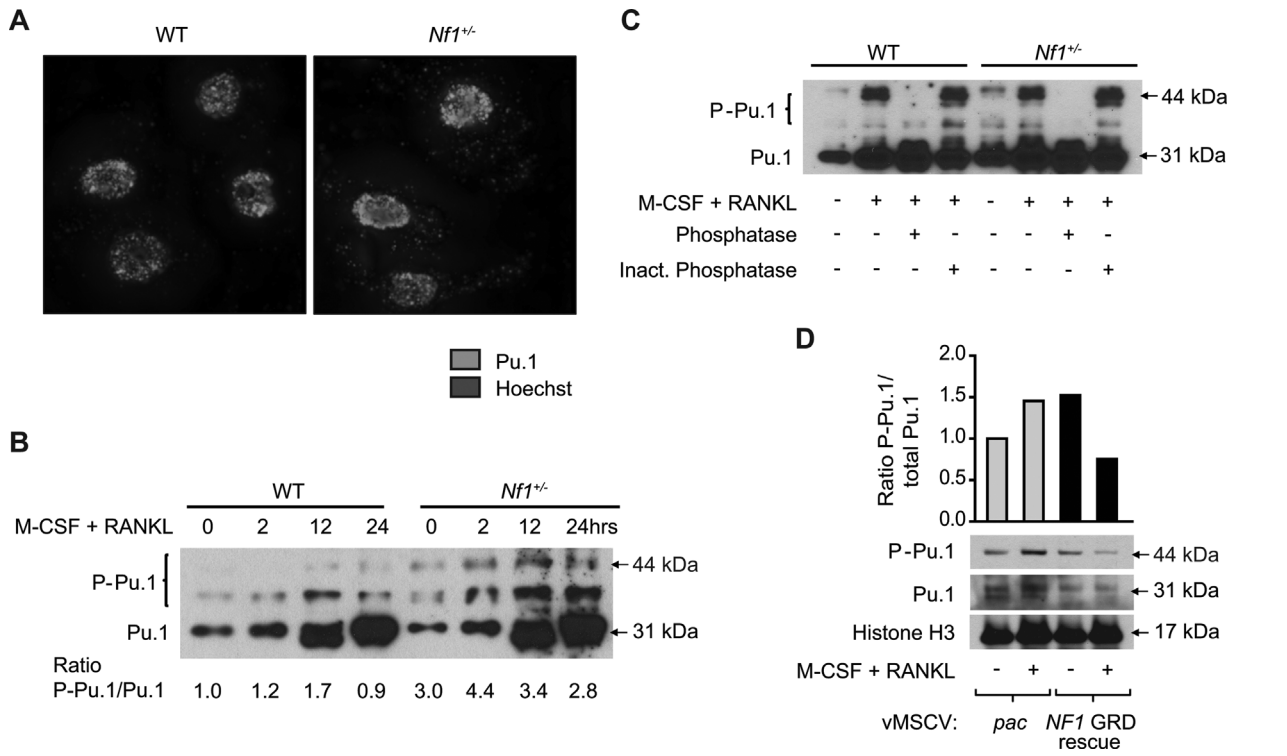

Fig. 4. *Nf1* haploinsufficiency drives p21-Ras–dependent phosphorylation of Pu.1 in the nucleus of myelomonocytic osteoclast precursors. Primary osteoclast progenitors were isolated from WT and *Nf1*$^{+/-}$ mice according to the same methodology as in previous experiments. (*A*) Representative photomicrographs of WT and *Nf1*$^{+/-}$ primary OC progenitors stained with FITC-labeled anti-Pu.1 (green) and Hoechst (blue). The assay was performed on two independent occasions with similar results. (*B*) Phosphorylated and nonphosphorylated Pu.1 species were detected in OC progenitor nuclear lysates by Western blot following stimulation with M-CSF and RANKL for 0, 2, 12, and 24 hours. The expression level of the phosphorylated Pu.1 species was determined by densitometry as a ratio to the predominant non-phosphorylated Pu.1 band as in internal nuclear loading control. This experiment was repeated three times, with similar results. (*C*) Nuclear protein lysates were prepared from OC progenitors following 12 hours of stimulation with M-CSF and RANKL. Nuclear lysates were subsequently incubated at 37 °C with either phosphatase or heat-inactivated phosphatase for a duration of 30 min prior to immunoblotting with anti-Pu.1 antibody. This experiment was performed two times, with similar results. (*D*) The human full-length GRD of *NF1* was re-expressed by retroviral transduction of primary c-kit^{+} hematopoietic cells isolated from the bone marrow of WT and *Nf1*$^{+/-}$ mice. After puromycin selection, cells were stimulated with M-CSF and RANKL and phosphorylated and nonphosphorylated Pu.1 species were detected in nuclear lysates by Western blot. Histone H3 was detected as an additional nuclear loading control. The ratio of phosphorylated to total Pu.1 was determined by densitometry. This experiment was performed twice, with similar results. OC = osteoclast; M-CSF = macrophage-colony stimulating factor; MSCV = murine stem cell virus; GRD = GTPase-activation protein–related domain; RANKL = receptor activator of NF-κB ligand; FITC = fluorescein isothiocyanate.

osteolytic activity in vivo following OVX-mediated proresorptive challenge. By contrast, *Nf1-Ctsk* mice did not recapitulate any of these phenotypes in analogous experiments, indicating a critical requirement for *Nf1* haploinsufficiency at a more primitive stage of myeloid development in perpetuating osteolytic activity.

Pu.1 transcriptional activity is indispensable for myelomonocytic and OC differentiation, whereby the absence of Pu.1 in mice leads to severe osteopetrosis and combined deficiency of both macrophages and OCs secondary to impaired expression of the M-CSF receptor, c-Fms.[35,45] Intriguingly, however, supraphysiologic levels of Pu.1 expression do not necessarily correlate with increased myelomonocytic lineage commitment. In fact, recent studies suggest that phosphorylation of Pu.1 plays a central role in modulating its DNA binding affinity,[37,46] and is thereby critical to its ability to activate myeloid-specific gene programs that promote terminal differentiation.[39,40] For instance, although human myeloid leukemic cell lines have been shown to overexpress Pu.1,[47] the transcript levels of Pu.1-dependent myeloid genes, such as *CD11b* and *c-fms*, are relatively low by comparison.[48,49] Carey and colleagues[37] showed that this discrepancy between Pu.1 expression level and transcriptional activity depends on the phosphorylation status of Pu.1, whereby Pu.1 phosphorylation induced by tetradecanoylphorbol-13 acetate (TPA) led to growth arrest in leukemic cells. A recent study by Seshire and colleagues[40] further showed that Pu.1 dephosphorylation at serine residues by the leukemia-associated fusion protein promyelocytic leukemia/retinoic acid receptor alpha (X-RARα) inhibits Pu.1 promoter binding and transcription of *c-fms* among other myelomonocytic genes.

In the present study, we show that the *Nf1* tumor suppressor gene modulates nuclear levels of phosphorylated Pu.1 in myeloid OC progenitors, whereby M-CSF/RANKL induced p21Ras hyperactivation (in the context of *Nf1* haploinsufficiency) leads to increased levels of phospho-Pu.1 in the nucleus. Re-expression of the human full-length GAP related

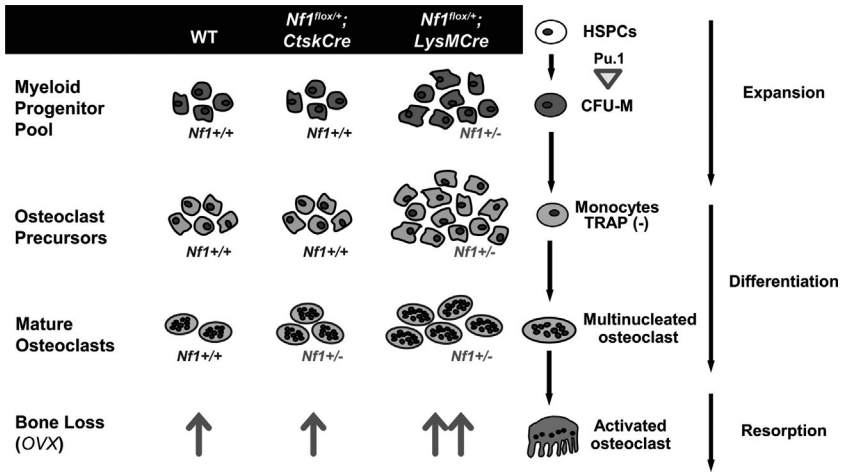

Fig. 5. Haploinsufficient loss of *Nf1* in myeloid progenitor cells is required to potentiate osteolytic activity in a mouse model of NF1-associated osteoporosis. Given that genetic ablation of a single *Nf1* allele in terminally differentiated osteoclasts alone (*Nf1-Ctsk*) is insufficient to augment the rate of bone lytic activity, we postulate that expansion of the OC precursor pool (*Nf1-LysM*) and an overall increase in OC numbers are the preponderant factors perpetuating excess osteolytic activity in vivo following OVX-mediated proresorptive challenge. These phenotypes are associated with p21-Ras–dependent hyperphosphorylation of the myeloid transcription factor Pu.1 in the nucleus of *Nf1* haploinsufficient myelomonocytic OC precursors. OC = osteoclast; OVX = ovariectomized/ovariectomy; HSPC = hematopoietic stem and progenitor cell; CFU-M = colony forming unit monocyte/macrophage; TRAP = tartrate-resistant acid phosphatase.

domain (GRD) of *NF1* in primary $Nf1^{+/-}$c-kit^{+} hematopoietic cells significantly attenuated the phosphorylation of nuclear Pu.1, showing the Ras-dependent nature of this process. The apparent association between increased phosphorylation of nuclear Pu.1 and enhanced osteoclastogenesis in the context of *Nf1* haploinsufficiency warrants further investigation in future studies.

Collectively, the results of this study suggest that the low bone mass phenotype observed in $Nf1^{+/-}$ and $Nf1^{-}$ *LysM* mice (and possibly the phenotype of osteopenia/osteoporosis in NF1 patients) may be due to enhanced OC differentiation and recruitment of OC progenitors, which occurs at a relatively primitive stage of myeloid differentiation, driven by Ras mediated hypersensitivity to M-CSF and RANKL. Thus, circumventing the early-stage recruitment and expansion of the OC progenitor pool by targeting the molecular pathways driving this process may represent a rational therapeutic strategy in the treatment of NF1-associated osteoporosis. By contrast, bisphosphonates, which have long been the clinical mainstay of in the treatment of osteoporosis, function to induce apoptosis of mature, terminally differentiated OCs as they begin to resorb the bone matrix. As they accumulate at high concentrations in the bone matrix, bisphosphonates have been associated with a number of deleterious effects over time, including the accumulation of microfractures and osteonecrosis among other complications.[50] These pitfalls have led to the advent of other novel antiresorptive therapies such as denosumab,[51] which acts at more primitive stage of OC development compared to bisphosphonates by blocking the RANKL-dependent terminal differentiation of OC progenitor cells.

Evidence regarding the efficacy of bisphosphonates in the treatment of NF1-associated osteoporosis are inconclusive. A recent clinical study limited to six patients with quite profound osteoporosis did demonstrate a trend toward increased BMD in five out of the six patients in the study, although the effect did not reach statistical significance after 23 months of treatment.[52] By contrast, recent work by Heervä and colleagues[53] has shown that OCs derived from human NF1 patients were resistant to bisphosphonate-induced apoptosis compared to healthy controls. As such, the application of targeted antiresorptive agents that act at a more primitive stage of OC differentiation may hold therapeutic promise in the treatment of NF1-associated osteopenia/osteoporosis and warrants further exploration in preclinical studies.

Disclosures

All authors state that they have no conflicts of interest.

Acknowledgments

This work was supported by the U.S. Department of Defense (DOD) (NF043032 to FCY; NF073112 to FCY; Children's Tumor Foundation (2011-01-010 to SDR); and Indiana Clinical and Translational Sciences Institute PHS NCCR (5TL1RR025759-03 to SDR). We thank Heather Daniel for administrative support.

Authors' roles: Study design: SDR, ZL, MX, and FCY. Study conduct: SDR, HY, RD, KM, YH, ZL, SC, KWS, LJ, XW, XY, XP, KSM, and TAG. Data analysis and interpretation: SDR, HY, RD, YH, ZL, and KWS. Drafting manuscript: SDR and FCY. Revising manuscript content: SDR, KSM, MX, and FCY. Approving final version of manuscript: FCY.

References

1. Roodman GD. Cell biology of the osteoclast. Exp Hematol. 1999;27(8):1229–41.

2. Teitelbaum SL, Ross FP. Genetic regulation of osteoclast development and function. Nat Rev Genet. 2003;4(8):638–49.
3. Tolar J, Teitelbaum SL, Orchard PJ. Osteopetrosis. N Engl J Med. 2004;351(27):2839–49.
4. Cackowski FC, Anderson JL, Patrene KD, et al. Osteoclasts are important for bone angiogenesis. Blood. 2010;115(1):140–9.
5. Mansour A, Abou-Ezzi G, Sitnicka E, Jacobsen SE, Wakkach A, Blin-Wakkach C. Osteoclasts promote the formation of hematopoietic stem cell niches in the bone marrow. J Exp Med. 2012;209(3):537–49.
6. Blin-Wakkach C, Rouleau M, Wakkach A. Roles of osteoclasts in the control of medullary hematopoietic niches. Arch Biochem Biophys. 2014 Nov 1;561: 29–37.
7. Yoshida H, Hayashi S, Kunisada T, et al. The murine mutation osteopetrosis is in the coding region of the macrophage colony stimulating factor gene. Nature. 1990;345(6274):442–4.
8. Lacey DL, Timms E, Tan HL, et al. Osteoprotegerin ligand is a cytokine that regulates osteoclast differentiation and activation. Cell. 1998;93(2):165–76.
9. Yasuda H, Shima N, Nakagawa N, et al. Osteoclast differentiation factor is a ligand for osteoprotegerin/osteoclastogenesis-inhibitory factor and is identical to TRANCE/RANKL. Proc Natl Acad Sci U S.A. 1998;95(7):3597–602.
10. Marks SC Jr, Seifert MF, McGuire JL. Congenitally osteopetrotic (oplop) mice are not cured by transplants of spleen or bone marrow cells from normal littermates. Metab Bone Dis Relat Res. 1984;5-(4):183–6.
11. Takeshita S, Namba N, Zhao JJ, et al. SHIP-deficient mice are severely osteoporotic due to increased numbers of hyper-resorptive osteoclasts. Nat Med. 2002;8(9):943–9.
12. Friedman JM, Gutmann DH, MacCollin M, Riccardi VM. Neurofibromatosis: phenotype, natural history, and pathogenesis. 3rd ed. Baltimore, MD: The Johns Hopkins University Press 1999.
13. Clark GJ, Drugan JK, Terrell RS, et al. Peptides containing a consensus Ras binding sequence from Raf-1 and theGTPase activating protein NF1 inhibit Ras function. Proc Natl Acad Sci U S.A. 1996;93(4): 1577–81.
14. Yang FC, Ingram DA, Chen S, et al. Nf1-dependent tumors require a microenvironment containing Nf1+/- and c-kit-dependent bone marrow. Cell. 2008;135(3):437–48.
15. Lammert M, Kappler M, Mautner VF, et al. Decreased bone mineral density in patients with neurofibromatosis 1. Osteoporos Int. 2005;16(9):1161–6.
16. Kuorilehto T, Poyhonen M, Bloigu R, Heikkinen J, Vaananen K, Peltonen J. Decreased bone mineral density and content in neurofibromatosis type 1: lowest local values are located in the load-carrying parts of the body. Osteoporos Int. 2005;16(8):928–36.
17. Dulai S, Briody J, Schindeler A, North KN, Cowell CT, Little DG. Decreased bone mineral density in neurofibromatosis type 1: results from a pediatric cohort. J Pediatr Orthop. 2007;27(4):472–5.
18. Yilmaz K, Ozmen M, Bora Goksan S, Eskiyurt N. Bone mineral density in children with neurofibromatosis 1. Acta Paediatr. 2007;96-(8):1220–2.
19. Stevenson DA, Moyer-Mileur LJ, Murray M, et al. Bone mineral density in children and adolescents with neurofibromatosis type 1. J Pediatr. 2007;150(1):83–8.
20. Tucker T, Schnabel C, Hartmann M, et al. Bone health and fracture rate in individuals with neurofibromatosis 1 (NF1). J Med Genet. 2009;46(4):259–65.
21. Heervä E, Koffert A, Jokinen E, et al. A controlled register-based study of 460 neurofibromatosis 1 patients: increased fracture risk in children and adults over 41 years of age. J Bone Miner Res. 2012;27:2333–7.
22. Yang FC, Chen S, Robling AG, et al. Hyperactivation of p21ras and PI3K cooperate to alter murine and human neurofibromatosis type 1-haploinsufficient osteoclast functions. J Clin Invest. 2006;116-(11):2880–91.
23. Heervä E, Alanne MH, Peltonen S, et al. Osteoclasts in neurofibromatosis type 1 display enhanced resorption capacity, aberrant morphology, and resistance to serum deprivation. Bone. 2010;47-(3):583–90.
24. Stevenson DA, Yan J, He Y, et al. Multiple increased osteoclast functions in individuals with neurofibromatosis type 1. Am J Med Genet A. 2011; 155A(5): 1050–9.
25. Li H, Liu Y, Zhang Q, et al. Ras dependent paracrine secretion of osteopontin by Nf1+/- osteoblasts promote osteoclast activation in a neurofibromatosis type I murine model. Pediatr Res. 2009;65(6):613–8.
26. Rhodes SD, Wu X, He Y, et al. Hyperactive transforming growth factor-beta1 signaling potentiates skeletal defects in a neurofibromatosis type 1 mouse model. J Bone Miner Res. 2013 Dec;28(12): 2476–89.
27. Elefteriou F, Benson MD, Sowa H, et al. ATF4 mediation of NF1 functions in osteoblast reveals a nutritional basis for congenital skeletal dysplasiae. Cell Metab. 2006;4(6):441–51.
28. Clausen BE, Burkhardt C, Reith W, Renkawitz R, Forster I. Conditional gene targeting in macrophages and granulocytes using LysMcre mice. Transgenic Res. 1999;8(4):265–77.
29. Chiu WS, McManus JF, Notini AJ, Cassady AI, Zajac JD, Davey RA. Transgenic mice that express Cre recombinase in osteoclasts. Genesis. 2004;39(3):178–85.
30. Zhu Y, Romero MI, Ghosh P, et al. Ablation of NF1 function in neurons induces abnormal development of cerebral cortex and reactive gliosis in the brain. Genes Dev. 2001;15(7):859–76.
31. Wu X, Chen S, He Y, et al. The haploinsufficient hematopoietic microenvironment is critical to the pathological fracture repair in murine models of neurofibromatosis type 1. PLoS One. 2011;6(9): e 24917.
32. Boyle WJ, Simonet WS, Lacey DL. Osteoclast differentiation and activation. Nature. 2003;423(6937):337–42.
33. Yan J, Chen S, Zhang Y, et al. Rac1 mediates the osteoclast gains-in-function induced by haploinsufficiency of Nf1. Hum Mol Genet. 2008;17(7):936–48.
34. Yu X, Chen S, Potter OL, et al. Neurofibromin and its inactivation of Ras are prerequisites for osteoblast functioning. Bone. 2005;36-(5):793–802.
35. Tondravi MM, McKercher SR, Anderson K, et al. Osteopetrosis in mice lacking haematopoietic transcription factor PU.1. Nature. 1997;386-(6620):81–4.
36. Delgado MD, Hallier M, Meneceur P, Tavitian A, Moreau-Gachelin F. Inhibition of Friend cells proliferation by spi-1 antisense oligodeoxynucleotides. Oncogene. 1994;9(6):1723–7.
37. Carey JO, Posekany KJ, deVente JE, Pettit GR, Ways DK. Phorbol ester-stimulated phosphorylation of PU.1: association with leukemic cell growth inhibition. Blood. 1996;87(10):4316–24.
38. Hiatt KK, Ingram DA, Zhang Y, Bollag G, Clapp DW. Neurofibromin GTPase-activating protein-related domains restore normal growth in Nf1-/- cells. J Biol Chem. 2001;276(10):7240–5.
39. Hamdorf M, Berger A, Schule S, Reinhardt J, Flory E. PKCdelta-induced PU. 1 phosphorylation promotes hematopoietic stem cell differentiation to dendritic cells. Stem Cells. 2011;29(2):297–306.
40. Seshire A, Rossiger T, Frech M, Beez S, Hagemeyer H, Puccetti E. Direct interaction of PU.1 with oncogenic transcription factors reduces its serine phosphorylation and promoter binding. Leukemia. 2012;26(6):1338–47.
41. Illes T, Halmai V, de Jonge T, Dubousset J. Decreased bone mineral density in neurofibromatosis-1 patients with spinal deformities. Osteoporos Int. 2001;12(10):823–7.
42. Alanne MH, Siljamäki E, Peltonen S, et al. Phenotypic characterization of transgenic mice harboring Nf1(+/-) or Nf1(-/-) osteoclasts in otherwise Nf1(+/+) background. J Cell Biochem. 2012 Jun;113(6): 2136–46.
43. Bollag G, Clapp DW, Shih S, et al. Loss of NF1 results in activation of the Ras signaling pathway and leads to aberrant growth in haematopoietic cells. Nat Genet. 1996;12(2):144–8.
44. Largaespada DA, Brannan CI, Jenkins NA, Copeland NG. Nf1 deficiency causes Ras-mediated granulocyte/macrophage colony stimulating factor hypersensitivity and chronic myeloid leukaemia. Nat Genet. 1996;12(2):137–43.
45. Scott EW, Simon MC, Anastasi J, Singh H. Requirement of transcription factor PU.1 in the development of multiple hematopoietic lineages. Science. 1994;265(5178):1573–7.

46. Pongubala JM, Van Beveren C, Nagulapalli S, et al. Effect of PU.1 phosphorylation on interaction with NF-EM5 and transcriptional activation. Science. 1993;259(5101):1622–5.
47. Hromas R, Orazi A, Neiman RS, et al. Hematopoietic lineage- and stage-restricted expression of the ETS oncogene family member PU.1. Blood. 1993;82(10):2998–3004.
48. Voso MT, Burn TC, Wulf G, Lim B, Leone G, Tenen DG. Inhibition of hematopoiesis by competitive binding of transcription factor PU.1. Proc Natl Acad Sci U S.A. 1994;91(17):7932–6.
49. Sariban E, Mitchell T, Kufe D. Expression of the c-fms proto-oncogene during human monocytic differentiation. Nature. 1985;316(6023):64–6.
50. Xu XL, Gou WL, Wang AY, et al. Basic research and clinical applications of bisphosphonates in bone disease: what have we learned over the last 40 years? J Transl Med. 2013;11:303.
51. McClung MR, Lewiecki EM, Cohen SB, et al. Denosumab in postmenopausal women with low bone mineral density. N Engl J Med. 2006;354(8):821–31.
52. Heervä E, Huilaja L, Leinonen P, Peltonen S, Peltonen J. Follow-up of six patients with neurofibromatosis 1-related osteoporosis treated with alendronate for 23 months. Calcif Tissue Int. 2014;94(6):608–12.
53. Heervä E, Peltonen S, Svedstrom E, Aro HT, Vaananen K, Peltonen J. Osteoclasts derived from patients with neurofibromatosis 1 (NF1) display insensitivity to bisphosphonates in vitro. Bone. 2012;50(3):798–803.